

pubs.acs.org/acsapm Article

Functionalized Thiophene-Based Aptasensors for the Electrochemical Detection of Mucin-1

Grace Haya, Damilola O. Runsewe, Mackenzie U. Otakpor, Gabriel E. Pohlman, Adelyne Towne, Tania Betancourt, and Jennifer A. Irvin*



Cite This: ACS Appl. Polym. Mater. 2023, 5, 1208-1218



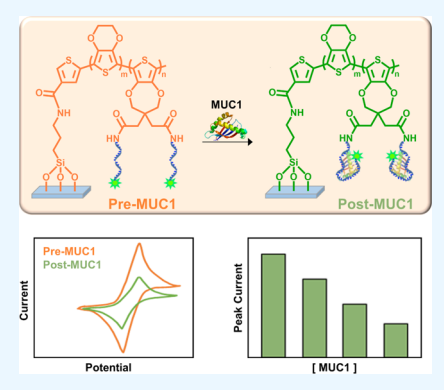
ACCESS I

III Metrics & More

Article Recommendations

Supporting Information

ABSTRACT: Mucin-1 (MUC1) is a glycoprotein found in epithelial tissues; its function is to protect the body by blocking pathogens from reaching the cells. Overexpression and elevated serum levels of this protein are observed in breast cancer, lung cancer, stomach cancer, ovarian cancer, and many other types of malignancies. Current methods used to detect cancer are expensive and therefore not readily accessible; some methods are also invasive. The ability to detect MUC1 could allow for early detection of cancer, leading to more successful outcomes. This research focuses on the development of a robust biosensor platform based on aptamer-functionalized electroactive polymers (EAPs) that can be used for the detection of cancer. To achieve this, indium tin oxide slide surfaces were modified to enable the electrochemical growth of an electroactive copolymer of 3,4-ethylenedioxythiophene (EDOT) and 2,2-(3,4-dihydro-2H-thieno[3,4-b][1,4]dioxepine-3,3-diyl)diacetic acid (ProDOT(COOH)₂), with the carboxylic acid functionalities added to introduce bonding sites for a MUC1-specific aptamer. Three copolymer ratios were



investigated to maximize the performance. The aptamer was then attached to the EAPs to create aptasensors that could be used for the electrochemical detection of a MUC1 polypeptide. The limits of detection of the biosensors and their stabilities were evaluated. The MUC1 aptasensor showed stability for at least 6 days, depending on the ratio of the copolymer, when stored in 0.1 M phosphate-buffered saline. The 1:2 EDOT/ProDOT(COOH)₂ copolymer was found to be the most stable over time and to offer one of the smallest limits of detection, making it the most favorable ratio for aptasensor optimization. Specifically, the 1:2 EDOT/ProDOT(COOH)₂ biosensor provided a limit of detection of 369 fg/mL (418 fM) and a linear range of 625 fg/mL to 6.25 ng/mL (709 fM to 7.09 nM) with the MUC1 peptide APDTRPAPG. The sensor also showed selectivity when tested with competing agents including IgG and cell media. The performance of the aptasensor demonstrated its potential as a highly sensitive and selective biosensor for MUC1 detection.

KEYWORDS: conducting polymer, aptamer, biosensor, electrochemical detection, mucin-1, cyclic voltammetry, PEDOT

1. INTRODUCTION

Mucins are a family of high molecular weight and heavily glycosylated proteins that are produced by epithelial tissues. They are generally classified into two families known as membrane-bound mucins and secreted (gel forming) mucins.^{1,2} Mucins are an important component in most gel-like secretions, thereby functioning as lubricants, cell signaling molecules, and chemical barrier components.^{2,3} Mucin-1 (MUC1) is the most studied mucin. It consists of a hydrophobic membrane-spanning domain, an extracellular domain at its N-terminus, and a cytoplasmic domain at its C-terminus, all of which are associated with each other through hydrogen bonding.^{1,4} MUC1 lines the surface of epithelial tissues in the stomach, eyes, lungs, and other organs. MUC1 protects the body from pathogens by stopping them from reaching the surface of the cells.⁶ This occurs by binding these pathogens to the oligosaccharides on the side chains of the MUC1 structure.

The overexpression of MUC1 has been found to be linked to breast, lung, bladder, ovarian, pancreatic, and stomach cancers. ^{1,2,6,8–13} In cancer cells, the glycosylation of MUC1 is truncated, affecting signaling pathways involved in malignancy. ^{2,6,14} Soluble MUC1, also known as cancer antigen 15-3 (CA 15-3), can typically be found in low-concentration levels (<31 U/mL) in healthy human serum. ¹⁵ Low levels of the MUC1 epitopes' cancer antigens 27-29 (CA 27-29 MUC1) and CA 15-3 in serum under 40 U/mL ¹⁶ and 35 U/mL, ¹⁷ respectively, are considered normal. Levels higher than these are indicative of malignancy. ¹⁸ A higher order of magnitude increase (up to 100-fold) in the amount of MUC1 is present in

Received: October 3, 2022 Accepted: January 1, 2023 Published: January 20, 2023





cancer cells when compared to normal cells.¹⁹ Budiu et al. discussed that MUC1 overexpression in treatment-resistant tumors largely mirrored elevated serum MUC1 levels (>35 U/mL, CA 15-3 test); soluble MUC1 levels average 1556 U/mL in the case of ovarian cancer.¹⁷ Persistently increased soluble MUC1 levels were also found to correlate with poor survival prognosis.¹⁷

The correlation between MUC1-derived "cancer antigen epitopes" and patient prognosis is therefore a critical element of cancer screening. Indeed, serial CA 15-3 measurements are commonly used to detect early recurrence and monitor metastatic breast cancer patients during follow-up. 20-24 Traditional methods such as enzyme-linked immunosorbent assay, dot blotting, western blotting, immunofluorescence, and immunohistochemistry have been utilized for the detection of MUC1,²⁵ but they are time-consuming, labor-intensive, and require a high level of expertise and dedicated instrumentation, therefore limiting their use in real-time, point-of-care clinical diagnostics. 26,27 For widespread adoption of MUC1-based screening of cancer, it is important to develop novel sensors for the rapid, sensitive, and selective detection of MUC1. Electrochemical detection methods have been researched in recent years as a good alternative to more traditional methods of biological detection due to their ease of use, rapid response, and high selectivity and sensitivity. $^{28-30}$

Electroactive polymers (EAPs) undergo reversible changes in the oxidation state that are accompanied by changes in properties such as color, conductivity, size, and reactivity, enabling their use in a wide variety of sensor applications. These polymers are composed of an extensive network of conjugated double bonds that allow for electron delocalization, reducing oxidation potentials. Electrons are removed from neutral EAPs during oxidation (p-doping) to introduce multiple cations (holes) along the backbone; electrons are returned to the polymers during reduction, returning the polymers to their neutral state (Figure 1). The redox behavior of EAPs has been thoroughly discussed elsewhere. Because the oxidation and reduction behavior of EAPs are very sensitive to changes in the environment, EAPs can be used as electrochemical sensors.

In combination with biorecognition molecules such as aptamers (APT), EAPs can be used as biosensing devices (Figure 2).³⁵ Aptamers are oligonucleotides (single-stranded DNA or RNA) that bind to a target molecule with high affinity and specificity.³⁶ Based on their affinity to the target molecule, they are selected from a library of random oligonucleotides by the SELEX (systematic evolution of ligands by exponential enrichment) method. The SELEX method for the selection of aptamers was first discussed by Gold³⁷ and by Ellington and Szoztak.³⁸

The research presented herein builds on our prior demonstration of an aptasensor for the detection of adenosine.³⁹ We have developed a biosensor that can be used to detect cancer by detecting the overexpression of MUC1 using EAPs. We electrochemically deposited a conductive copolymer made up of different ratios of 3,4-ethylenedioxythiophene (EDOT) and 2,2-(3,4-dihydro-2*H*-thieno[3,4-*b*][1,4]dioxepine-3,3-diyl)diacetic acid (ProDOT-(COOH)₂) repeat units. To ensure robust performance, the copolymers were covalently bonded to the electrodes. The MUC1 aptamer was then attached to the carboxylic acid moieties of ProDOT(COOH)₂ to provide the aptasensors specificity toward MUC1. Utilizing cyclic voltammetry, we

$$-e^{-\frac{1}{2}} + e^{-\frac{1}{2}}$$

$$-e^{-\frac{1}{2}} + e^{-\frac{1}{2}}$$

Figure 1. Alternating double and single bonds in EAPs such as PEDOT allow it to undergo reversible oxidation and reduction processes, forming resonance-delocalized electrons and cations (holes) along the backbone.³¹ Addition and removal of electrons causes interconversion between neutral polymers (top), radical cations known as polarons (middle), and dications known as bipolarons (bottom). Adapted with permission from Runsewe, D.; Betancourt, T.; Irvin, J.A. Biomedical Application of EAPs in Electrochemical Sensors: A Review. *Materials* (*Basel*)2019, 12, 2629. Copyright 2019 MDPI.

investigated the response of the aptasensors to the presence of a MUC1 peptide. The limits of detection, linear ranges, and stabilities of the aptasensors were determined.

2. EXPERIMENTAL METHODS

2.1 Reagents and Materials. Platinum (Pt) button working electrodes (MF-2013; 1.6 mm diameter) were purchased from Bioanalytical Systems, Inc. (West Lafayette, IN, USA). Indium tin oxide (ITO)-coated glass slides (CG-50IN-CUV: $8-12~\Omega$) were purchased from Delta Technologies (Loveland, CO, USA). Tetrabutylammonium perchlorate (TBAP) was purchased from TCI Chemicals (Portland, OR, USA). TBAP was recrystallized from ethyl acetate or ethanol and dried under vacuum prior to use. ITO-coated slides were soaked in 1.0 M HCl for approximately 10 s, then soaked with purified water twice, and dried with lint-free wipes. The slides were then washed with acetone and dried with lint-free wipes. Anhydrous acetonitrile was purchased from Acros Organics (New Jersey, USA). N-Hydroxysuccinimide (NHS), 3-thiophenecarboxylic acid (3-Th-COOH), and ethanol (95%) were purchased from Thermo Fisher Scientific (Waltham, MA, USA) and used as received. 3-(Aminopropyl)triethoxysilane (APTES) (98%) and 1-ethyl-3-(3dimethylaminopropyl)-carbodiimide (EDC) were purchased from Alfa Aesar (Haverhill, MA, USA) and used as received. PProDOT-(COOH)₂ was synthesized and purified as per a literature procedure.⁴⁰ EDOT was purchased from Acros Organics (Waltham, MA, USA) and purified as per a literature procedure. 41 Phosphatebuffered saline (PBS) (10x) was purchased from SeraCare (Milford, MA, USA). This buffer was diluted to 1× with autoclaved water to obtain a 0.1 M PBS buffer (150 mM NaCl, 10 mM sodium phosphate, pH 7.4). Ultrapure deionized water was obtained from a Millipore Direct Q system (18.2 M Ω). Immunoglobulin G 2B (purified mouse IgG2B, catalog number MAB004) was purchased from R&D Systems (Minneapolis, MA, USA) and resuspended in 0.1 M PBS. Dulbecco's

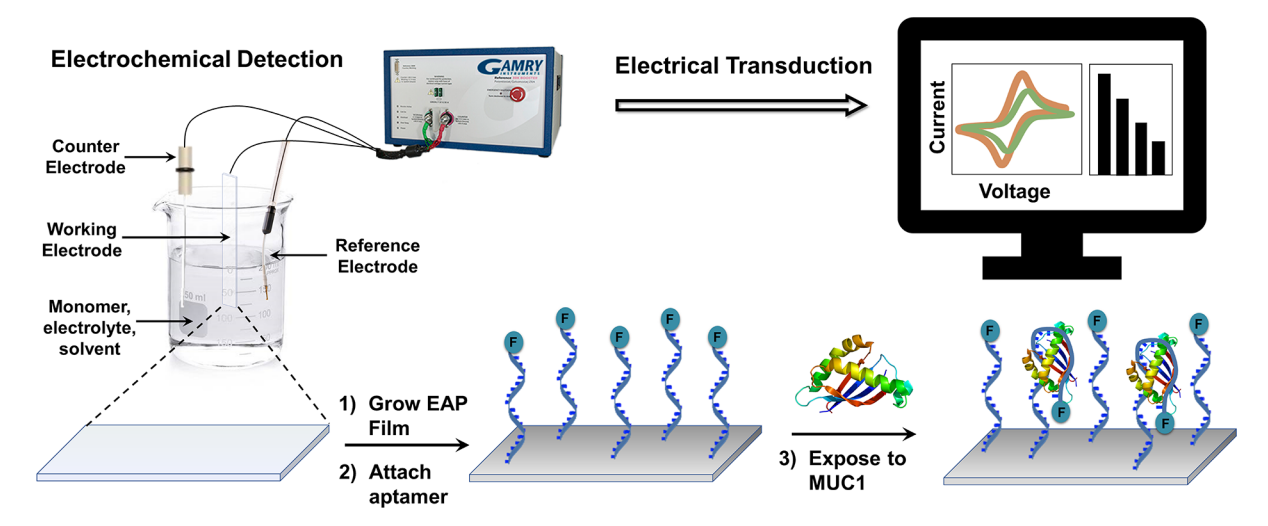


Figure 2. Biomolecule detection scheme.

modified Eagle's medium cell culture medium was purchased from Corning Inc. (Corning, NY, USA). All reagents were used as received unless specifically stated otherwise.

A MUC1 aptamer was purchased from Integrated DNA Technologies (Coralville, IA, USA). This aptamer binds to a common 9 amino-acid-long peptide sequence (APDTRPAPG) of the variable tandem repeat domain epitope within the highly immunogenic region of MUC1. 42 The sequence of the aptamer is

5'-/56FAM/GCA GTT GAT CCT TTG GAT ACC CTG GTT TTT/3AmMO/-3'.

Here, AmMO represents an amino linker, and FAM represents fluorescein amidite. The aptamer was dissolved in autoclaved ultrapure water to a stock concentration of 1000 μ M, aliquoted into autoclaved centrifuge tubes, and stored in a -25 °C freezer. PBS was also autoclaved prior to use with the oligonucleotide.

The MUC1 peptide APDTRPAPG (MW. 880.96 g/mol) was procured from Anaspec (Freemont, CA, USA).

2.2. Instrumentation. All electrochemical measurements were performed using cyclic voltammetry on a Pine WaveNow potentiostat. The setup consisted of a three-electrode system. The working electrode was a Pt button electrode or an ITO-coated glass slide. A Pt flag was used as the counter electrode. The reference electrode for aqueous electrochemical characterization and detection was a Ag/ AgCl electrode (CH Instruments, Inc., Bee Cave, TX, USA), while a Ag/Ag+ reference electrode was used for the electrochemical growth of the polymers in acetonitrile (CH₃CN). The Ag/Ag⁺ reference electrode was prepared as follows: a non-aqueous reference electrode body was fitted with a CoralPor tip (Bioanalytical Systems Inc., West Lafayette, IN, USA) and filled with a 0.01 M AgNO₃, 0.1 M TBAP solution in acetonitrile. A silver wire was then immersed in the solution, and the electrode was stored with the tip immersed in 0.1 M TBAP in acetonitrile. All cyclic voltammograms (CVs) were acquired at a scan rate of 100 mV/s. A fluorescence microscope (Invitrogen EVOS FL digital fluorescence microscope) was utilized to obtain fluorescence images of the immobilized aptamer by using the GFP setting on the fluorescent microscope ($\lambda_{EX} = 470/22$ nm, $\lambda_{EM} = 525/$ 50 nm). The images were captured at a light intensity of 50%, a shutter speed of 1 ns, and at a magnification of 20x.

Absorbance and fluorescence spectroscopy measurements were carried out with a BioTek Synergy H4 hybrid microplate reader using a Take3 accessory to position the samples. Attenuated total reflectance—infrared (ATR-IR) spectroscopic analyses were accomplished using a Bruker Tensor II Fourier transform—infrared (FTIR) spectrometer fitted with a Harrick SplitPea attenuated total reflectance accessory.

2.3. Electrochemical Copolymerization on Platinum Button Electrodes. Mixed monomer solutions composed of different ratios of EDOT and $ProDOT(COOH)_2$ in 0.1 M TBAP in acetonitrile were

prepared using the following EDOT/ProDOT(COOH)₂ co-monomer molar ratios: 2:1 (33% ProDOT(COOH)₂), 1:1 (50% ProDOT(COOH)₂), and 1:2 (67% ProDOT(COOH)₂); each solution was made with a total combined monomer concentration of 0.01 M. The EAP films were then electrochemically deposited onto a Pt button using CV with a Ag/Ag⁺ reference electrode and a Pt flag counter electrode at a scan rate of 100 mV/s for three cycles. Potential windows used varied with co-monomer ratios as can be seen in the Supporting Information (Figure S1).

2.4. ITO Slide Modification, Copolymer Growth, and Copolymer Stability. A 3-Th-COOH-modified ITO-coated slide was used as a working electrode to grow the poly(3,4-ethylenedioxythiophene) (PEDOT)-co-PProDOT-(COOH)₂ copolymers. The ITO-coated slides were modified with APTES and 3-Th-COOH to ensure covalent attachment of the polymer to the substrate (Figure 3) as we previously described³⁹ and according to a procedure developed by Thermo Scientific.⁴³

Mixed monomer solutions composed of different ratios of EDOT and ProDOT(COOH)₂ in 0.1 M TBAP in acetonitrile were prepared using three co-monomer molar ratios: 1:1, 1:2, and 2:1 EDOT/ProDOT(COOH)₂ with a total combined monomer concentration of 0.01 M (Figure 3). In order to test the effect of monomer concentration on film stability, an additional experiment was conducted using 0.0025 M EDOT and 0.0025 M ProDOT(COOH)₂. The EAP films were then electrochemically deposited onto the modified slides using CV with a Ag/Ag⁺ reference electrode and a Pt flag counter electrode at a scan rate of 100 mV/s from -1.2 to 1.7 V for three cycles.

The cycling stability of the 1:2 EDOT/ProDOT(COOH) $_2$ copolymer film was investigated over 100 cycles by cycling in 0.1 M PBS from -1.2 to 0.6 V at a scan rate of 100 mV/s. The current response of the copolymer film over these cycles was compared.

2.5. Aptamer Attachment. For this research, the MUC1 aptamer was attached to the carboxylic acid functionalized EAP by pipetting PBS containing 25 mg/mL EDC, 30 mg/mL NHS, and 30 μ M of the aptamer onto the top of the slide and incubating for 2.5 h at room temperature. The resulting aptasensor was washed extensively with PBS to remove excess aptamer from the electrode surface. Figure 3 illustrates the process of attaching the aptamer to the polymer. Aptamer attachment to the copolymer on the ITO slide was confirmed using CV, fluorescence microscopy, and infrared spectroscopy. CVs of the copolymer were acquired before and after aptamer attachment using a potential sweep at 100 mV s⁻¹ from -1.2 to 0.6 V in 0.1 M PBS and a Ag/AgCl reference electrode.

Fluorescence microscopy was used to examine the PBS-wetted slides by imaging the FAM label of the aptamer. Fluorescence images of the aptamer's FAM label ($\lambda_{\rm Ex}=495~{\rm nm}$ and $\lambda_{\rm Em}=520~{\rm nm}$) were captured using an Invitrogen EVOS FL microscope at a light intensity

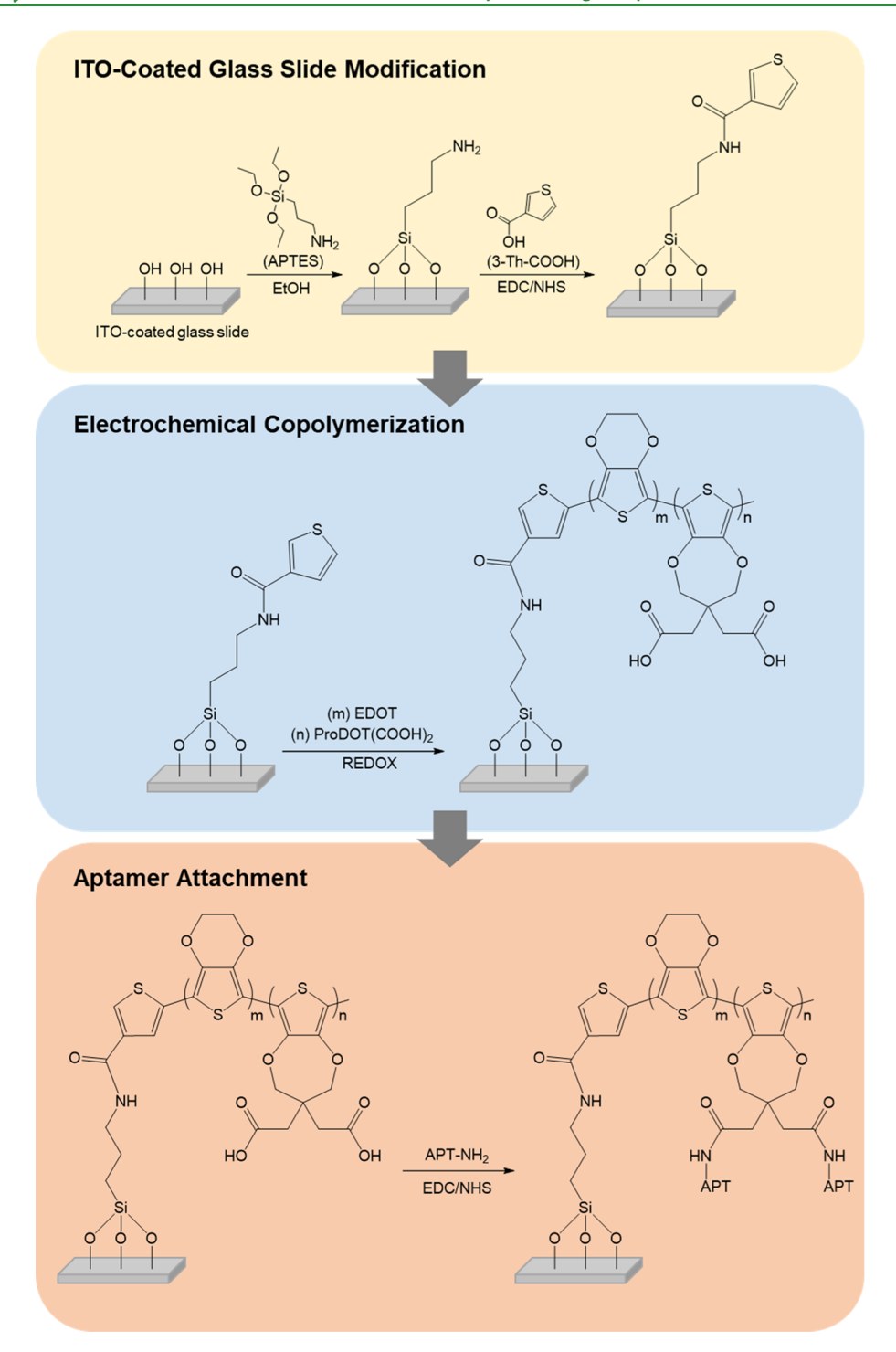


Figure 3. ITO-coated glass slide modification, electrochemical copolymerization, and aptamer attachment.

of 50%, a shutter speed of 1 ns, and at a magnification of $20\times$ using a GFP filter cube (470/22 nm excitation and 525/50 nm emission). Two controls were used on substrates with a ratio of 1:2 EDOT/ProDOT(COOH)₂ to demonstrate the sensing specificity provided by the presence of the aptamer. The negative control lacked the aptamer. Instead, the EAP substrate was exposed to only PBS (pH 7.4). The second control consisted of an adsorption control where the EAP was exposed to the aptamer without the use of EDC and NHS.

Attenuated total reflectance infrared spectra were acquired using a thiophene carboxylate-modified ITO slide, a 1:2 EDOT/ProDOT-(COOH)₂ copolymer film electrochemically deposited on the modified ITO, and an aptamer-functionalized copolymer film on the modified ITO to confirm the functionalization of the biosensor.

2.6. Electrochemical Detection of the MUC1 Antigen. The performance of the MUC1 aptasensor was investigated by incubating it in increasing concentrations of MUC1 peptide in 0.1 M PBS (pH 7.4) in the concentration range shown in Table 1 for 30 min per concentration.

After incubation, the MUC1 solution was wicked away with a lint-free wipe, and the MUC1-bound aptasensor was characterized using cyclic voltammetry in 0.1 M PBS with a potential window of -1.2 to 0.6 V with a Ag/AgCl reference electrode and a Pt flag counter electrode at a scan rate of 100 mV/s. The current at the polymer oxidation peak potential for each concentration was used to determine the limit of detection (LOD) and linear range of the aptasensor. Three CVs were obtained for each concentration to calculate the

Table 1. Concentration of MUC1 Peptide Solutions Used for Evaluating Sensor Performance

solution no.	peptide concentration
0	0 fg/mL
1	625 fg/mL(709 fM)
2	6.25 pg/mL(7.09 pM)
3	62.5 pg/mL(70.9 pM)
4	625 pg/mL(709 M)
5	6.25 ng/mL(7.09 nM)
6	62.5 ng/mL(70.9 nM)
7	625 ng/mL(709 nM)
8	6.25 μ g/mL(7.09 μ M)
9	12.5 μ g/mL(14.2 μ M)
10	$25 \ \mu g/mL(28.4 \ \mu M)$
11	$50 \ \mu \text{g/mL} (56.8 \ \mu \text{M})$
12	100 μ g/mL(113.5 μ M)

standard deviation. The LOD was calculated as the concentration at which the sensor's signal was three standard deviations from that of the blank, per eq 1

$$Signal_{LOD} = signal_{blank} - 3 \cdot \sigma_{blank}$$
 (1)

where $\sigma_{\rm blank}$ represents the standard deviation between replicates of the blank.

The negative control EAP biosensor lacking the MUC1 aptamer was exposed to the same range of concentrations of MUC1 peptide for comparison.

2.7. Determination of Sensor Specificity and Stability. The interference of the various non-specific targets was tested by incubating the MUC1 aptasensor along with a mixture of the non-complimentary targets: IgG and cell culture media. The detection was characterized using CV. A two-tailed, paired Student's t-test was utilized to determine the statistical significance of differences between samples with interfering agents and the control. p < 0.05 was set as the significance level.

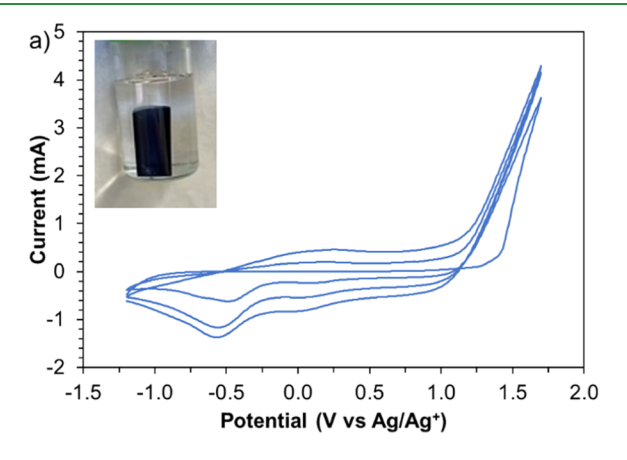
The storage electrochemical stability of the aptasensor was investigated over a period of 10 days. The aptasensor was stored in 0.1 M PBS, and CVs were obtained every 2 days. In addition, the stability for the 1:2 EDOT/ProDOT(COOH)₂ copolymer ratio was also tested on day 7 and day 14 while keeping the biosensor stored in PBS.

3. RESULTS

3.1. Polymer Growth and Cycling Stability. Direct covalent attachment of aptamers to an EAP substrate is facilitated using the ProDOT-(COOH)₂ monomer; the carboxylic acid groups can be further decorated with aptamers via amide linkages as shown in Figure 3. As reported previously,³⁹ the water solubility of the ProDOT-(COOH)₂ homopolymer makes it unsuitable for aptasensor use. Instead, electrochemical polymerization of a 1:2 ratio of EDOT/ProDOT(COOH)₂ yields a stable, insoluble copolymer that could be bonded to an aptamer for analyte detection.

In this work, other monomer ratios have been explored to identify the best combination of insolubility and functionalizability for optimal MUC1 aptasensor performance. Many instances of electrochemical copolymerization can be found in the literature, but best results are generally found when oxidation potentials of the two monomers are within ca. 0.2 V of each other. 44 In the case of the copolymers explored here, EDOT oxidizes at 0.92 V versus Ag/Ag⁺ on a Pt button working electrode, while ProDOT(COOH), oxidizes at 1.15 V versus Ag/Ag+, a difference of 0.23 V. The electrochemical copolymerization of the two monomers was explored at 0, 33, 50, 67, and 100% ProDOT(COOH)2. In all cases other than 100% ProDOT(COOH)₂, polymerization onset was apparent beginning at 0.92 V versus Ag/Ag⁺ (Figure S1) on a platinum button electrode, consistent with EDOT oxidation. Interestingly, the current response for PProDOT(COOH)₂ deposition is much lower than that for PEDOT deposition, possibly indicating that either less polymerization occurs with ProDOT-(COOH), or that PProDOT(COOH), is less electroactive than PEDOT. In the copolymers, the current response decreased as the ProDOT(COOH)₂ content increased (Figure S1).

For aptasensor fabrication and testing, the Pt button working electrodes were replaced with ITO-coated glass slides; the much larger surface area of the ITO slides increases the oxidation potential somewhat to 1.28 V versus Ag/Ag⁺ for all the three ratios used (1:2, 1:1, and 2:1 EDOT/ProDOT-(COOH)₂). The CV for the 1:2 ratio of EDOT/ProDOT-(COOH)₂ can be seen in Figure 4a; CVs for the other ratios are similar and can be found in the Supporting Information (Figure S2). Electrochemical copolymerization for all ratios



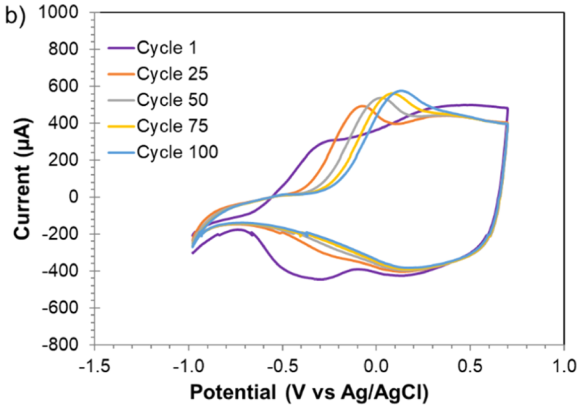


Figure 4. (a) CV of copolymer growth for the 1:2 ratio of EDOT/ProDOT(COOH)₂ (total monomer concentration 0.01 M in 0.1 M TBAP in acetonitrile) on an ITO-coated glass slide at 100 mV/s from -1.2 to +1.7 V vs Ag/Ag⁺. Inset: Image of copolymer growth on a modified ITO-coated glass slide stored in the oxidized state in acetonitrile. (b) Polymer cycling stability: the 1:2 EDOT:ProDOT(COOH)₂ copolymer film was cycled from -1.2 to 0.6 V 100 times in 0.1 M PBS at a scan rate of 100 mV/s.

resulted in the formation of deep blue films (Figure 4a inset) that were insoluble in acetonitrile.

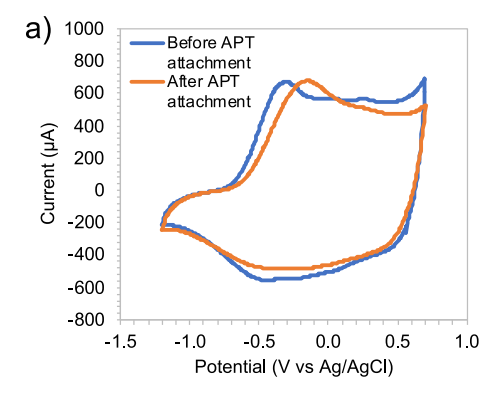
The cycling stability of the 1:2 EDOT/ProDOT(COOH)₂ copolymer film was tested by cycling it from -1.2 to 0.6 V for 100 cycles. As can be seen in Figure 4b, the shapes of the CVs shift, with each subsequent oxidation sharpening and the oxidation peak shifting to a slightly higher potential; the most pronounced change occurs in the first 25 cycles. From this plot, it is evident that the film did not delaminate or lose electroactivity, even after 100 cycles. The change in oxidation behavior may be due to the switch from the organic TBAP electrolyte solution to the aqueous PBS electrolyte solution; changing electrolyte has been observed to change the electrochemical behavior. 45,46

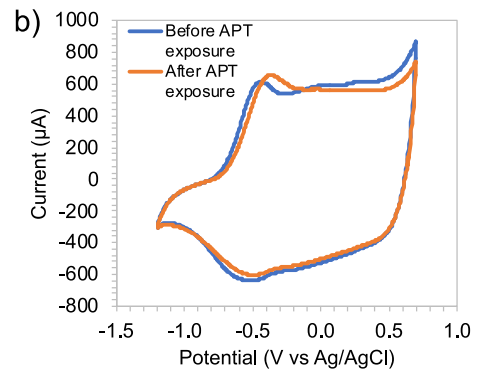
3.2. Aptamer Attachment to the EAP Biosensor. Figure 5a shows the CV of the copolymer film before and after MUC1 aptamer covalent attachment with EDC and NHS on a biosensor with the 1:2 PEDOT/PProDOT(COOH)₂ copolymer ratio, while Figure S3 (Supporting Information) shows the CVs for the 1:1 and 2:1 ratios. For all the three copolymer ratios, there was a slight positive shift in the peak oxidation potential and a slight negative shift in the peak reduction potential after aptamer attachment. The data suggest that addition of the non-conductive aptamer to the surface results in increased driving voltage requirements to enable polymer oxidation or reduction.

The adsorption control (Figure 5b) consisted of a 1:2 EDOT/ProDOT(COOH)₂ copolymer film exposed to the MUC1 aptamer without EDC and NHS. The negative control (Figure 5c) consisted of a 1:2 EDOT/ProDOT(COOH)₂ copolymer film exposed to PBS but no aptamer. Both controls show only minor changes in the oxidation and reduction peaks before and after the copolymer films were exposed to the aptamer without EDC and NHS (Figure 5b) or PBS (Figure 5c). The changes observed in these controls were smaller than those observed when the aptamer was attached (Figure 4a) and could at least in part be attributed to the shifts observed with running CV on the sample, as observed in Figure 3b.

Fluorescence microscopy was also used to confirm aptamer attachment to the biosensor surfaces. Figure 6a shows fluorescence microscopy images of the biosensor with the 1:2 PEDOT/PProDOT(COOH)₂ copolymer ratio after attachment of the aptamer. Green fluorescence associated with the fluorescein tag on the 5' end of the aptamer confirmed the presence of the aptamer. Images of the negative control do not show any fluorescence, as expected, since no aptamer was attached to the copolymer (Figure 6b). Images of the adsorption control showed the presence of some fluorescence due to nonspecific adsorption of the aptamer (Figure 6c). The small band gap of 1:2 PEDOT/PProDOT-(COOH)₂ (1.85 eV; Figure S4) leads to rapid electron-hole recombination, rendering these polymers natively nonfluorescent. ⁴⁷Figure S5 shows the lack of fluorescence of the copolymer in the excitation wavelength range of 300-550 nm, confirming the lack of overlap with fluorescein. Thus, the only source of fluorescence in these films is the fluorescein fluorescent label of the aptamer.

Infrared spectroscopy was also used to provide evidence of aptamer attachment. The FTIR spectra of the modified ITO, the 1:2 EDOT/ProDOT(COOH)₂ copolymer grown on the modified ITO, and the aptamer-functionalized copolymer on the modified ITO can be seen in Figure S6. The copolymer spectrum is similar to that of PEDOT, 48 with the addition of





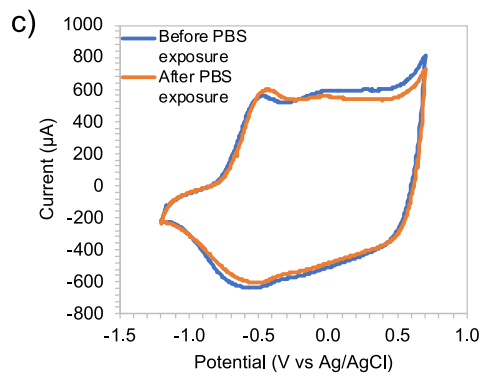


Figure 5. (a) CVs before and after MUC1 aptamer attachment for the biosensor with the 1:2 EDOT/ProDOT(COOH)₂ copolymer in the reduced state. Sensors show a slight shift to a higher potential for the oxidation peak and a slight decrease in the reduction peak after attachment. (b) Adsorption control: CVs from before and after the copolymer were exposed to the MUC1 aptamer without using EDC and NHS. (c) Negative control: CVs from before and after the copolymer was exposed to PBS only.

C=O absorption (centered around 1650 cm⁻¹). The notable differences going from the copolymer to the aptamer-functionalized copolymer are increased water content in the more hydrophilic aptamer-functionalized copolymer (broad absorption centered at 3204 cm⁻¹), an increase in the primary amide content due to C=N and additional amide groups in the aptamer (1627 cm⁻¹), increased absorption due to additional ether groups in the aptamer (1135 cm⁻¹), and increased absorption due to incorporation of P-O-C groups in the aptamer (ca. 1010 cm⁻¹).

3.3. Électrochemical Detection of the MUC1 Antigen. The aptasensors were incubated with the MUC1 peptide at varying concentrations for 30 min prior to wicking of the fluid and collection of CVs in PBS. Figure 7a—d shows the MUC1 detection conducted with the MUC1 polypeptide. As shown in

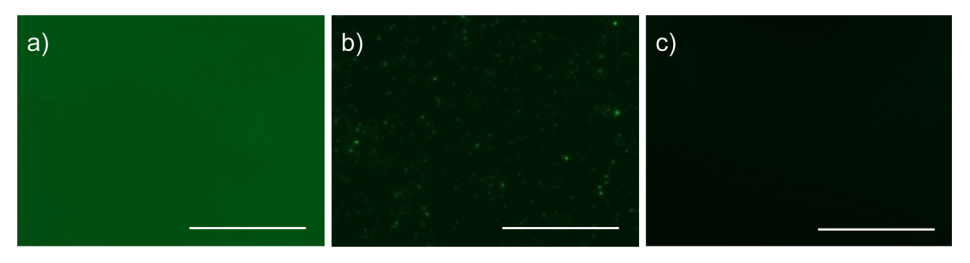


Figure 6. Fluorescence microscopy images (470/22 nm excitation and 525/50 nm emission) of (a) EAP + APT + EDC/NHS; (b) EAP + APT in the absence of EDC/NHS; and (c) EAP in the absence of APT, EDC, or NHS. EAP = EAP with 1:2 EDOT/ProDOT(COOH)₂ molar ratio; APT = aptamer. Green fluorescence observed in "a" is associated with the fluorescein amidite label of the aptamer, confirming its attachment to the EAP via carbodiimide chemistry. The low level of fluorescence in "b" indicates a mild level of aptamer adsorption to the EAP in the absence of EDC and NHS which prevent covalent attachment to the substrate. Scalebar = 200 μ m.

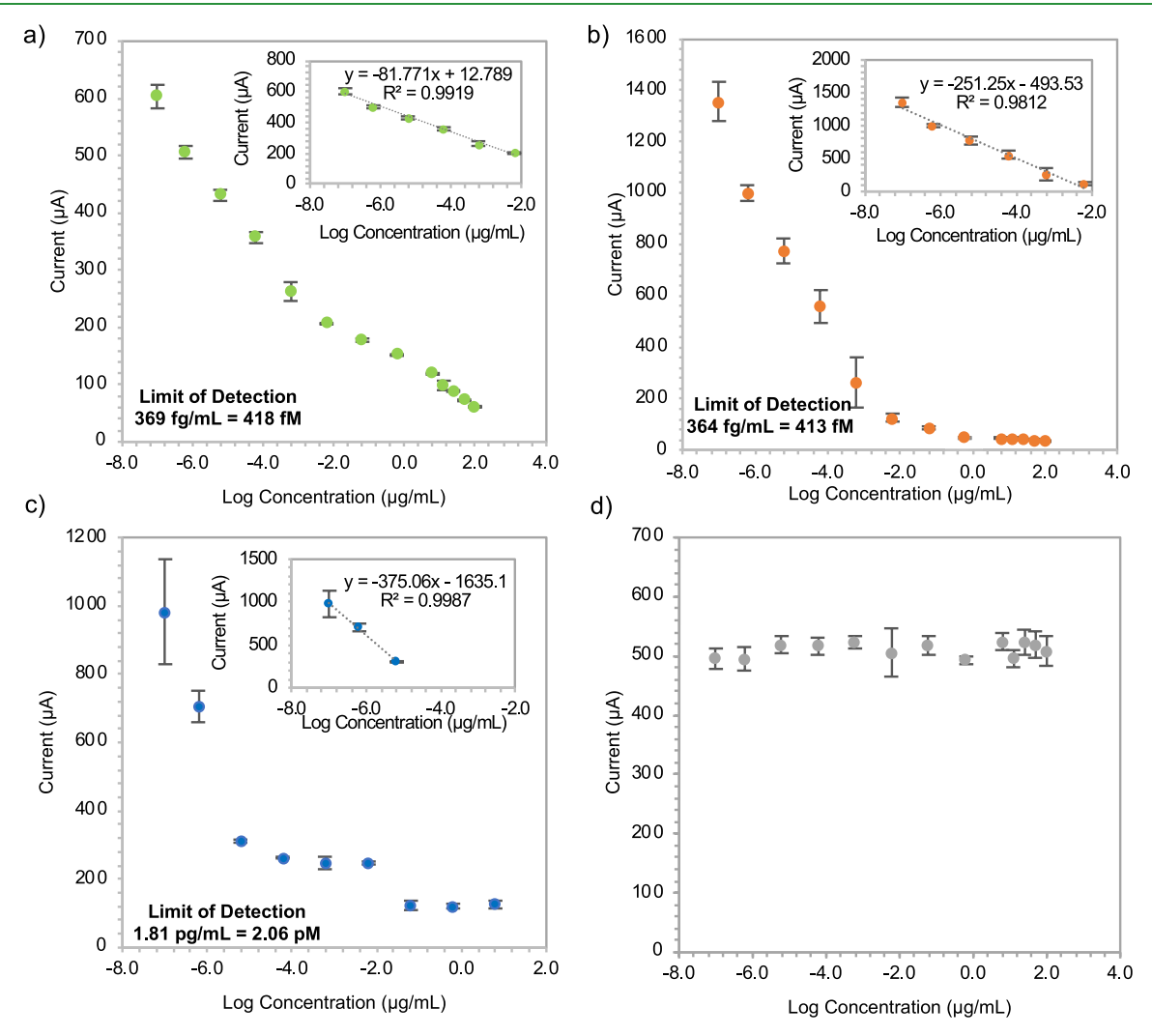


Figure 7. (a–c) Plot of response of biosensors with (a) 1:2 EDOT/ProDOT(COOH)₂, (b) 1:1 EDOT/ProDOT(COOH)₂, and (c) 2:1 EDOT/ProDOT(COOH)₂ ratios as a function of MUC1 peptide concentration (from 1 to 12: 625 fg/mL, 6.25 pg/mL, 62.5 pg/mL, 62.5 pg/mL, 62.5 pg/mL, 62.5 ng/mL, 62.5 ng/mL, 62.5 ng/mL, 62.5 ng/mL, 62.5 μ g/mL, 12.5 μ g/mL, 25 μ g/mL, 50 μ g/mL, and 100 μ g/mL) in 0.1 M PBS (pH 7.4). Inset: Plot of peak current ν s log of MUC1 peptide concentration in the linear range. (d) Plot of response of control biosensor lacking aptamer to MUC1 solutions at varying concentrations.

Figure 7a, the peak anodic current decreased with increasing concentrations of the MUC1 peptide. This may be caused by the addition of the negatively charged aptamer interacting with the non-conducting macromolecule (MUC1 peptide), thereby reducing the conductivity of the aptasensor and requiring more voltage to drive the ions through it. The reduction in electrochemical response of the aptasensor may be due to

the formation of the more aptamer—target complex, which increases the charge-transfer resistance of the aptasensor. Of note, interaction with the target MUC1 peptide results in a decrease in the oxidation peak current, that is, an opposite trend to that observed in Figure 4b upon cycling the polymer.

MUC1 detection using the biosensor prepared from the 1:2 EDOT/ProDOT(COOH)₂ copolymer ratio was linear from

Table 2. Comparison of Aptasensor Performance Obtained and Other MUC1 Aptasensors in the Literature

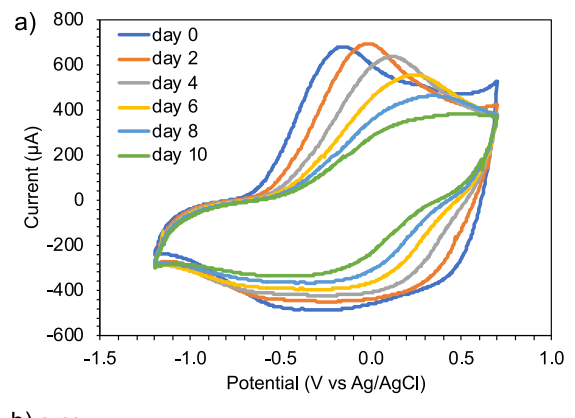
detection methods	analyte	linear range	LOD	reference
electrochemical impedance spectroscopy	MUC1 peptide (APDTRPAPG)	10 pg/mL to 1.0 μ g/mL	0.90 pg/mL	49
fluorescence	MUC1 peptide (APDTRPAPG)	5.31 ng/mL to 200 ng/mL	37.62 ng/mL	50
fluorescence	MUC1 protein	0.2 ng/mL to 100 ng/mL	0.13 ng/mL	51
electrochemical impedance spectroscopy (EIS) and differential pulse voltammetry (DPV)	MUC1 protein	3.6 ng/mL EIS and 0.95 ng/mL DPV	3.6 ng/mL EIS and 0.95 ng/mL DPV	52
CV, EIS, and DPV	MUC1 protein	1 fM to 100 nM	0.79 fM	53
fluorescence	MUC1 protein	50 pg/mL to 100 ng/mL	10 pg/mL	54
CV	MUC1 peptide	625 fg/mL to 6.25 ng/mL (709 fM to 7.09 nM)	369 fg/mL (418 fM)	this work

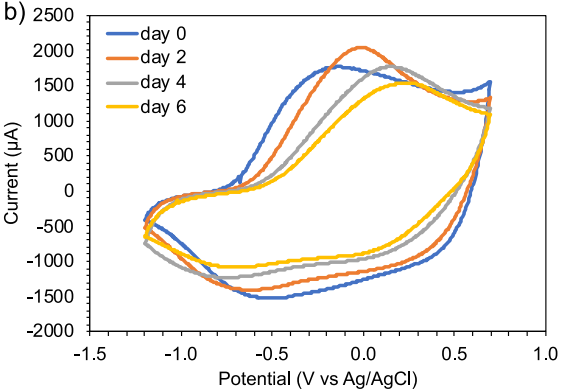
625 fg/mL to 6.25 ng/mL (709 fM to 7.09 nM) with a LOD of 369 fg/mL (418 fM) (Figure 7a). MUC1 detection for the biosensor prepared from the 1:1 EDOT/ProDOT(COOH)₂ copolymer ratio was similar, with a linear relationship from 625 fg/mL to 6.25 ng/mL (709 fM to 7.09 nM) and a LOD of 364 fg/mL (413 fM) (Figure 7b). Detection using the biosensor prepared from the 2:1 EDOT/ProDOT(COOH)₂ copolymer ratio was less effective, with a narrow linear relationship only from 625 fg/mL to 6.25 pg/mL (7.09 fM to 7.09 pM) and a LOD of 1.81 pg/mL (2.06 pM) (Figure 7c). Overall, the 2:1 EDOT/ProDOT(COOH)₂ copolymer ratio resulted in the largest LOD and the smallest linear range. Biosensors prepared from both the 1:1 EDOT/ProDOT(COOH)₂ and 1:2EDOT/ProDOT(COOH)₃ copolymer ratios were more favorable.

To demonstrate that the behavior observed was a direct result of capture of the target MUC1 by the aptasensor, we conducted a control study in which a CP-coated electrode lacking the aptamer was exposed to the same MUC1 solutions. Figure 7d shows that in the absence of an aptamer, no significant response is observed, as expected. This indicates that nonspecific adsorption of MUC1 on the CP surface does not significantly affect the sensor's performance.

The performance of the aptasensor reported in this work was compared to what was previously reported in the literature. Table 2 shows the performance of other aptasensors for the detection of MUC1, and the results of the aptasensor in this work are comparable in terms of low detection limit. The EAP-based aptasensor in this work provides a low LOD and broad linear range and has the benefit of a less-expensive immobilization matrix material (conducting polymer) that can be synthesized commercially for potential large-scale manufacturing of the aptasensor once all relevant parameters are optimized.

3.4. Aptasensor Stability. The stability of the biosensors prepared with each of the three copolymer ratios was tested by storing the biosensors in 0.1 M PBS at room temperature and subjecting them to CV measurements either every 2 days (Figure 8) or only on days 0, 7, and 14 (Figure 9). In all cases, the current response increased slightly between day 0 and the next measurement; this is likely a result of the copolymer films equilibrating to the new electrolyte. As can be seen in Figure 8, biosensors prepared from all the three ratios appeared to maintain the electrochemical stability for at least 6 days. Specifically, the sensor's current output was maintained within 20% of the original response after storage in PBS during this time period. Nonetheless, the oxidation peak potentials for all the three ratios did increase over time, indicative of loss of electroactivity which may be due to irreversible oxidation. This





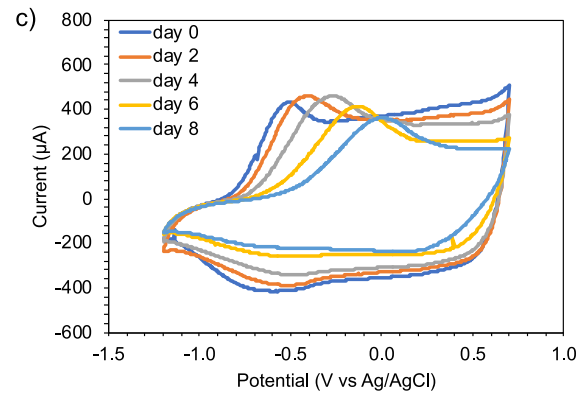
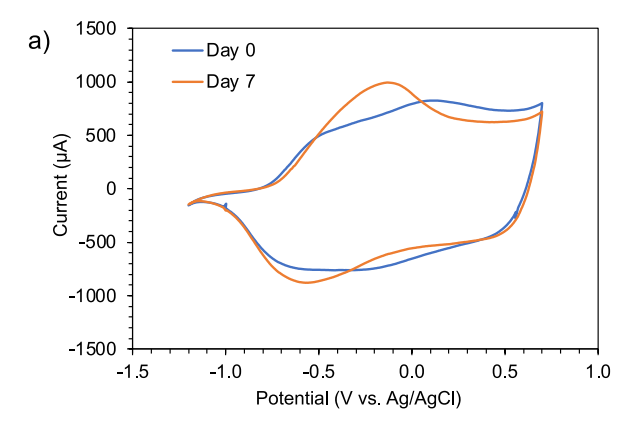


Figure 8. CVs reveal the stability of copolymer aptasensors every 2 days after incubation in 0.1 M PBS (pH 7.4). (a) 1:2 EDOT/ProDOT(COOH)₂, (b) 1:1 EDOT/ProDOT(COOH)₂, and (c) 2:1 EDOT/ProDOT(COOH)₂.

effect could potentially be mitigated by storing the biosensors under inert conditions prior to use, as we showed in our



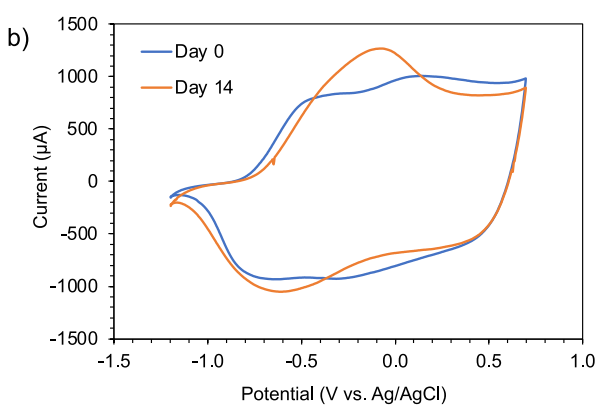


Figure 9. Storage stability studies examining the electrochemical response of the biosensor prepared using the 1:2 EDOT/ProDOT-(COOH)₂ copolymer ratio on (a) day 0 and day 7 and (b) day 0 and day 14.

previous work.³⁹ The 1:2 EDOT/ProDOT(COOH)₂ sensor maintained electroactivity for up to 10 days, while the 1:1 EDOT/ProDOT(COOH)₂ and the 2:1 EDOT/ProDOT-(COOH)₂ biosensors delaminated after 6 and 8 days, respectively. Taken in combination with the superior LOD and linear range seen in Figure 7, the biosensor prepared using 1:2 EDOT/ProDOT(COOH)₂ is clearly the best choice among the three biosensor ratios used in this study. As can be seen in Figure 9, the 1:2 biosensor was still stable after 7 days, and after 14 days; the replicates of these experiments (Figure S7) are consistent with the results seen in Figure 9.

3.5. Selectivity of the Aptasensor. A comparative study was conducted to investigate the selectivity of the aptasensor. This was achieved by incubating the aptasensor in 12.5 μ g/mL IgG and 1:20 dilution of cell culture media as the interfering molecules, both individually and combined. Cell culture media, an interfering matrix for this study, typically contains amino acids, vitamins, and carbohydrates that could potentially interfere with the MUC1 peptide. A 1:20 dilution of cell media was selected in accordance with the procedures previously reported in the literature. ^{50,51}Figure 10 shows the response of the aptasensor represented as a normalized percent change in peak current response. The formation of the targetaptamer complex causes a decrease in the charge transfer of the ions to the aptasensor surface. This leads to a significant change in the peak current response when compared to zero concentration, as can be seen with both MUC1 current responses in the figure. The interaction of the aptasensor with the cell culture media leads to a higher than background

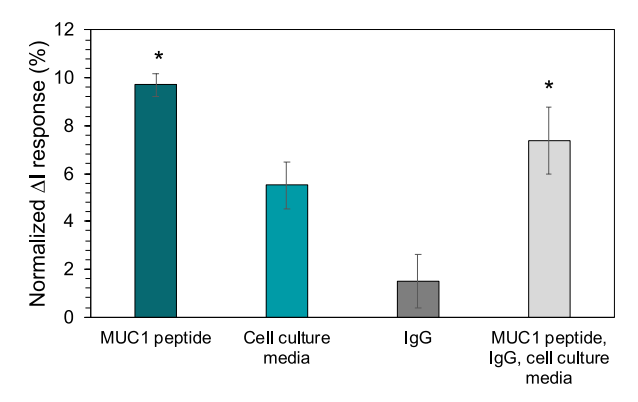


Figure 10. Selectivity of the aptasensor toward 12.5 μ g/mL MUC1 and interfering species IgG (12.5 μ g/mL) and cell culture media (1:20 dilution). * Statistically significant from the aptasensor change in current response at 0 concentration.

change in current response but significantly smaller than the samples that have MUC1 present.

The aptasensor showed very good selectivity against the IgG interfering molecule as very little change in current response was observed. The aptasensor was then incubated in a mixture of 1:20 dilution of cell culture media, 12.5 μ g/mL IgG, and 12.5 μ g/mL MUC1 (performed for each of the MUC1 peptides). The MUC1 mixtures containing interfering molecules showed good change in current response, which suggests that the aptasensor was able to successfully bind to the MUC1 target in the presence of the interfering molecules.

4. CONCLUSIONS

EAP-based electrochemical aptasensors were prepared as low-cost, rapid screening tests for MUC1. ProDOT(COOH)₂ was used as an electroactive monomer that provided sites for aptamer attachment in combination with EDOT used to impart the insolubility, and thus the stability, of the resultant aptasensors. Three different electroactive monomer ratios were used to prepare EAP copolymer aptasensors for MUC1, with a goal of maximizing sensitivity and stability. While both the 1:2 and 1:1 EDOT/ProDOT(COOH)₂ ratios produced similar low limits of detection (ca., 369 fg/mL or 418 fM) and broad linear ranges (625 fg/mL to 6.25 ng/mL) with the MUC1 peptide APDTRPAPG, the 1:2 ratio was found to be more stable. This 1:2 aptasensor was found to retain its electroactivity for at least 14 days when stored in a 0.1 M PBS solution.

The 1:2 aptasensor's selectivity was investigated with relevant interfering species such as IgG and cell culture media. The aptasensor was successfully able to selectively bind and show a significant change in the peak current response in the presence of the MUC1 target.

ASSOCIATED CONTENT

Supporting Information

The Supporting Information is available free of charge at https://pubs.acs.org/doi/10.1021/acsapm.2c01739.

CVs for electrochemical polymerization of different monomer ratios on platinum button electrodes; CVs for electrochemical polymerization on ITO-coated glass slides; CVs of 1:1 and 2:1 copolymers before and after aptamer attachment; UV—vis spectrum of the reduced 1:2 copolymer; emission spectra of the reduced and

oxidized 1:2 copolymer; FTIR spectra of the modified ITO glass slide, the modified slide coated with the 1:2 copolymer, and the aptamer-functionalized copolymer on the modified ITO; and replicates of CVs for 7 day and 14 day storage stability studies on aptasensors prepared using the 1:2 copolymer (PDF)

AUTHOR INFORMATION

Corresponding Authors

Tania Betancourt — Department of Chemistry and Biochemistry and Materials Science, Engineering and Commercialization Program, Texas State University, San Marcos, Texas 78748, United States; orcid.org/0000-0002-2460-6133; Email: tania.betancourt@txstate.edu

Jennifer A. Irvin — Department of Chemistry and Biochemistry and Materials Science, Engineering and Commercialization Program, Texas State University, San Marcos, Texas 78748, United States; orcid.org/0000-0003-3500-8419; Email: jennifer.irvin@txstate.edu

Authors

Grace Haya — Department of Chemistry and Biochemistry, Texas State University, San Marcos, Texas 78748, United States; © orcid.org/0000-0003-0498-2446

Damilola O. Runsewe – Materials Science, Engineering and Commercialization Program, Texas State University, San Marcos, Texas 78748, United States; ⊙ orcid.org/0000-0003-1813-9732

Mackenzie U. Otakpor – Department of Chemistry and Biochemistry, Texas State University, San Marcos, Texas 78748, United States

Gabriel E. Pohlman – Department of Chemistry and Biochemistry, Texas State University, San Marcos, Texas 78748, United States; orcid.org/0000-0003-0044-3285

Adelyne Towne – Department of Chemistry and Biochemistry, Texas State University, San Marcos, Texas 78748, United States

Complete contact information is available at: https://pubs.acs.org/10.1021/acsapm.2c01739

Author Contributions

§G.H. and D.O.R. contributed equally to this manuscript.

The authors declare no competing financial interest.

ACKNOWLEDGMENTS

This research was funded by the National Science Foundation Partnership for Research and Education in Materials, grant #2122041 and the NSF CheMIE REU grant #1757843. Additionally, D.R. received the Texas State University Doctoral Research Fellowship funding (grant #9000002701) in support of this research. The authors would also like to thank the reviewers for their many helpful suggestions.

REFERENCES

- (1) Bafna, S.; Kaur, S.; Batra, S. K. Membrane-bound mucins: the mechanistic basis for alterations in the growth and survival of cancer cells. *Oncogene* **2010**, *29*, 2893–2904.
- (2) Chugh, S.; Gnanapragassam, V. S.; Jain, M.; Rachagani, S.; Ponnusamy, M. P.; Batra, S. K. Pathobiological implications of mucin glycans in cancer: Sweet poison and novel targets. *Biochim. Biophys. Acta* **2015**, *1856*, 211–225.

- (3) Marin, F.; Luquet, G.; Marie, B.; Medakovic, D.Molluscan Shell Proteins: Primary Structure, Origin, and Evolution. In *Current Topics in Developmental Biology*; Academic Press, 2007; Vol. 80, pp 209–276.
- (4) Hu, R.; Wen, W.; Wang, Q.; Xiong, H.; Zhang, X.; Gu, H.; Wang, S. Novel electrochemical aptamer biosensor based on an enzyme-gold nanoparticle dual label for the ultrasensitive detection of epithelial tumour marker MUC1. *Biosens. Bioelectron.* **2014**, *53*, 384–389.
- (5) Nath, S.; Mukherjee, P. MUC1: a multifaceted oncoprotein with a key role in cancer progression. *Trends Mol. Med.* **2014**, *20*, 332–342.
- (6) Nath, S.; Mukherjee, P. MUC1: a multifaceted oncoprotein with a key role in cancer progression. *Trends Mol. Med.* **2014**, *20*, 332–342.
- (7) Baruch, A.; Hartmann, M.-l.; Yoeli, M.; Adereth, Y.; Greenstein, S.; Stadler, Y.; Skornik, Y.; Zaretsky, J.; Smorodinsky, N. I.; Keydar, I.; et al. The breast cancer-associated MUC1 gene generates both a receptor and its cognate binding protein. *Cancer Res.* 1999, 59, 1552–61
- (8) Kaur, S.; Momi, N.; Chakraborty, S.; Wagner, D. G.; Horn, A. J.; Lele, S. M.; Theodorescu, D.; Batra, S. K. Altered Expression of Transmembrane Mucins, MUC1 and MUC4, in Bladder Cancer: Pathological Implications in Diagnosis. *PLoS One* **2014**, *9*, No. e92742.
- (9) Saltos, A.; Khalil, F.; Smith, M.; Li, J.; Schell, M.; Antonia, S. J.; Gray, J. E. Clinical associations of mucin 1 in human lung cancer and precancerous lesions. *Oncotarget* **2018**, *9*, 35666–35675.
- (10) Lakshmanan, I.; Ponnusamy, M. P.; Macha, M. A.; Haridas, D.; Majhi, P. D.; Kaur, S.; Jain, M.; Batra, S. K.; Ganti, A. K. Mucins in Lung Cancer: Diagnostic, Prognostic, and Therapeutic Implications. *J. Thorac. Oncol.* **2015**, *10*, 19–27.
- (11) Wang, R. Q.; Fang, D. C. Alterations of MUC1 and MUC3 expression in gastric carcinoma: relevance to patient clinicopathological features. *J. Clin. Pathol.* **2003**, *56*, 378–384.
- (12) Deng, J.; Wang, L.; Chen, H.; Li, L.; Ma, Y.; Ni, J.; Li, Y. The role of tumour-associated MUC1 in epithelial ovarian cancer metastasis and progression. *Cancer Metastasis Rev.* **2013**, 32, 535–551.
- (13) Hinoda, Y.; Ikematsu, Y.; Horinochi, M.; Sato, S.; Yamamoto, K.; Nakano, T.; Fukui, M.; Suehiro, Y.; Hamanaka, Y.; Nishikawa, Y.; et al. Increased expression of MUC1 in advanced pancreatic cancer. *J. Gastroenterol.* **2003**, *38*, 1162–1166.
- (14) Movahedin, M.; Brooks, T. M.; Supekar, N. T.; Gokanapudi, N.; Boons, G.-J.; Brooks, C. L. Glycosylation of MUC1 influences the binding of a therapeutic antibody by altering the conformational equilibrium of the antigen. *Glycobiology* **2017**, *27*, *677*–*687*.
- (15) Moreno, M.; Bontkes, H. J.; Scheper, R. J.; Kenemans, P.; Verheijen, R. H. M.; von Mensdorff-Pouilly, S. High level of MUC1 in serum of ovarian and breast cancer patients inhibits huHMFG-1 dependent cell-mediated cytotoxicity (ADCC). *Cancer Lett.* **2007**, 257, 47–55.
- (16) Frenette, P. S.; Thirlwell, M. P.; Trudeau, M.; Thomson, D. M. P.; Joseph, L.; Shuster, J. S. The Diagnostic Value of CA 27-29, CA 15-3, Mucin-Like Carcinoma Antigen, Carcinoembryonic Antigen and CA 19-9 in Breast and Gastrointestinal Malignancies. *Tumor Biol.* 1994, 15, 247–254.
- (17) Budiu, R. A.; Mantia-Smaldone, G.; Elishaev, E.; Chu, T.; Thaller, J.; McCabe, K.; Lenzner, D.; Edwards, R. P.; Vlad, A. M. Soluble MUC1 and serum MUC1-specific antibodies are potential prognostic biomarkers for platinum-resistant ovarian cancer. *Cancer Immunol. Immunother.* 2011, 60, 975.
- (18) Alataş, F.; Alataş, Ö.; Metintaş, M.; Çolak, Ö.; Harmanci, E.; Demir, S. Diagnostic value of CEA, CA 15-3, CA 19-9, CYFRA 21-1, NSE and TSA assay in pleural effusions. *Lung Cancer.* **2001**, *31*, 9–16. (19) Apostolopoulos, V.; Pietersz, G. A.; Tsibanis, A.; Tsikkinis, A.; Drakaki, H.; Loveland, B. E.; Piddlesden, S. J.; Plebanski, M.; Pouniotis, D. S.; Alexis, M. N.; et al. Pilot phase III immunotherapy study in early-stage breast cancer patients using oxidized mannan-
- (20) Fehm, T.; Jäger, W.; Krämer, S.; Sohn, C.; Solomayer, E.; Wallwiener, D.; Gebauer, G. Prognostic Significance of Serum HER2

MUC1 [ISRCTN71711835]. Breast Cancer Res. 2006, 8, R27.

- and CA 15-3 at the Time of Diagnosis of Metastatic Breast Cancer. Anticancer Res. 2004, 24, 1987.
- (21) Jäger, W. The early detection of disseminated (metastasized) breast cancer by serial tumour marker measurements. *Eur. J. Cancer Prev.* **1993**, *2*, 133–139.
- (22) Hayes, D. F.; Zurawski, V. R.; Kufe, D. W. Comparison of circulating CA15-3 and carcinoembryonic antigen levels in patients with breast cancer. *J. Clin. Oncol.* **1986**, *4*, 1542–1550.
- (23) Safi, F.; Kohler, I.; Beger, H.-G.; Röttinger, E. The value of the tumor marker CA 15-3 in diagnosing and monitoring breast cancer. A comparative study with carcinoembryonic antigen. *Cancer* **1991**, *68*, 574–582.
- (24) Tondini, C.; Hayes, D. F.; Gelman, R.; Henderson, I. C.; Kufe, D. W. Comparison of CA15-3 and carcinoembryonic antigen in monitoring the clinical course of patients with metastatic breast cancer. *Cancer Res.* **1988**, *48*, 4107–12.
- (25) Yousefi, M.; Dehghani, S.; Nosrati, R.; Zare, H.; Evazalipour, M.; Mosafer, J.; Tehrani, B. S.; Pasdar, A.; Mokhtarzadeh, A.; Ramezani, M. Aptasensors as a new sensing technology developed for the detection of MUC1 mucin: A review. *Biosens. Bioelectron.* **2019**, 130, 1–19.
- (26) Wang, Z.; Xia, N.; Shi, J.; Li, S.; Zhao, Y.; Wang, H.; Liu, L. Electrochemical Aptasensor for Determination of Mucin 1 by P-Aminophenol Redox Cycling. *Anal. Lett.* **2014**, *47*, 2431–2442.
- (27) Zhang, N.; Li, W.; Guo, Z.; Sha, Y.; Wang, S.; Su, X.; Jiang, X. Electrochemiluminescence Aptasensor for the MUC1 Protein Based on Multi-functionalized Graphene Oxide Nanocomposite. *Electroanalysis* **2016**, 28, 1504–1509.
- (28) Mahato, K.; Purohit, B.; Bhardwaj, K.; Jaiswal, A.; Chandra, P. Novel electrochemical biosensor for serotonin detection based on gold nanorattles decorated reduced graphene oxide in biological fluids and in vitro model. *Biosens. Bioelectron.* **2019**, *142*, 111502.
- (29) Wang, X.; Su, J.; Zeng, D.; Liu, G.; Liu, L.; Xu, Y.; Wang, C.; Liu, X.; Wang, L.; Mi, X. Gold nano-flowers (Au NFs) modified screen-printed carbon electrode electrochemical biosensor for label-free and quantitative detection of glycated hemoglobin. *Talanta* 2019, 201, 119–125.
- (30) Yang, Y.; Fu, Y.; Su, H.; Mao, L.; Chen, M. Sensitive detection of MCF-7 human breast cancer cells by using a novel DNA-labeled sandwich electrochemical biosensor. *Biosens. Bioelectron.* **2018**, *122*, 175–182.
- (31) Runsewe, D.; Betancourt, T.; Irvin, J. A. Biomedical Application of Electroactive Polymers in Electrochemical Sensors: A Review. *Materials* **2019**, *12*, 2629.
- (32) K, K.; Rout, R. Conducting polymers: a comprehensive review on recent advances in synthesis, properties and applications. *RSC Adv.* **2021**, *11*, 5659–5697.
- (33) Le, T. H.; Kim, Y.; Yoon, H. Electrical and Electrochemical Properties of Conducting Polymers. *Polymers* **2017**, *9*, 150.
- (34) Tajik, S.; Beitollahi, H.; Nejad, F. G.; Shoaie, I. S.; Khalilzadeh, M. A.; Asl, M. S.; Van Le, Q.; Zhang, K.; Jang, H. W.; Shokouhimehr, M. Recent developments in conducting polymers: applications for electrochemistry. *RSC Adv.* **2020**, *10*, 37834–37856.
- (35) Runsewe, D.; Betancourt, T.; Irvin, J. A. Biomedical Application of Electroactive Polymers in Electrochemical Sensors: A Review. *Materials* **2019**, *12*, 2629.
- (36) Sun, H.; Zhu, X.; Lu, P. Y.; Rosato, R. R.; Tan, W.; Zu, Y. Oligonucleotide Aptamers: New Tools for Targeted Cancer Therapy. *Mol. Ther. Nucleic Acids* **2014**, *3*, No. e182.
- (37) Tuerk, C.; Gold, L. Systematic evolution of ligands by exponential enrichment: RNA ligands to bacteriophage T4 DNA polymerase. *Science* **1990**, 249, 505–510.
- (38) Ellington, A. D.; Szostak, J. W. In vitro selection of RNA molecules that bind specific ligands. *Nature* **1990**, *346*, 818–822.
- (39) Runsewe, D. O.; Haya, G.; Betancourt, T.; Irvin, J. A. Conducting Polymer-Based Electrochemical Aptasensor for the Detection of Adenosine. ACS Appl. Polym. Mater. 2021, 3, 6674–6683.

- (40) Beaujuge, P. M.; Amb, C. M.; Reynolds, J. R. A Side-Chain Defunctionalization Approach Yields a Polymer Electrochrome Spray-Processable from Water. *Adv. Mater.* **2010**, *22*, 5383–5387.
- (41) Winkel, K. L.; Carberry, J. R.; Irvin, J. A. Synthesis and Electropolymerization of 3,5-Bis-(3,4-ethylenedioxythien-2-yl)-4,4-dimethyl Isopyrazole: A Donor-Acceptor-Donor Monomer. *J. Electrochem. Soc.* 2013, 160, G111–G116.
- (42) Ferreira, C. S. M.; Matthews, C. S.; Missailidis, S. DNA Aptamers That Bind to MUC1 Tumour Marker: Design and Characterization of MUC1-Binding Single-Stranded DNA Aptamers. *Tumor Biol.* **2006**, *27*, 289–301.
- (43) Tech Tip # 5: Attach an antibody onto glass, silica or quartz surface. http://tools.thermofisher.com/content/sfs/brochures/TR0005-Attach-Ab-glass.pdf. Accessed December 13, 2022.
- (44) Li, C.; Liu, C.; Shi, L.; Nie, G. Electrochemical copolymerization of 3,4-ethylenedioxythiophene and 6-cyanoindole and its electrochromic property. *J. Mater. Sci.* **2015**, *50*, 1836–1847.
- (45) Aydemir, N.; Kilmartin, P. A.; Travas-Sejdic, J.; Kesküla, A.; Peikolainen, A.-L.; Parcell, J.; Harjo, M.; Aabloo, A.; Kiefer, R. Electrolyte and solvent effects in PPy/DBS linear actuators. *Sens. Actuators, B* **2015**, 216, 24–32.
- (46) Irvin, J. A.; Carberry, J. R. Dominant ion transport processes of ionic liquid electrolyte in poly(3,4-ethylenedioxythiophene). *J. Polym. Sci., Part B: Polym. Phys.* **2013**, *51*, 337–342.
- (47) Prasad, K. P.; Chen, Y.; Sk, M. A.; Than, A.; Wang, Y.; Sun, H.; Lim, K.-H.; Dong, X.; Chen, P. Fluorescent quantum dots derived from PEDOT and their applications in optical imaging and sensing. *Mater. Horiz.* **2014**, *1*, 529–534.
- (48) Zhao, Q.; Jamal, R.; Zhang, L.; Wang, M.; Abdiryim, T. The structure and properties of PEDOT synthesized by template-free solution method. *Nanoscale Res. Lett.* **2014**, *9*, 557.
- (49) Wang, M.; Hu, B.; Ji, H.; Song, Y.; Liu, J.; Peng, D.; He, L.; Zhang, Z. Aptasensor Based on Hierarchical Core-Shell Nanocomposites of Zirconium Hexacyanoferrate Nanoparticles and Mesoporous mFe3O4@mC: Electrochemical Quantitation of Epithelial Tumor Marker Mucin-1. ACS Omega 2017, 2, 6809–6818.
- (50) Wang, W.; Wang, Y.; Pan, H.; Cheddah, S.; Yan, C. Aptamerbased fluorometric determination for mucin 1 using gold nanoparticles and carbon dots. *Microchim. Acta* **2019**, *186*, 544.
- (51) Li, Z.; Mao, G.; Du, M.; Tian, S.; Niu, L.; Ji, X.; He, Z. A fluorometric turn-on aptasensor for mucin 1 based on signal amplification via a hybridization chain reaction and the interaction between a luminescent ruthenium(II) complex and CdZnTeS quantum dots. *Microchim. Acta* 2019, 186, 233.
- (52) Florea, A.; Taleat, Z.; Cristea, C.; Mazloum-Ardakani, M.; Săndulescu, R. Label free MUC1 aptasensors based on electrodeposition of gold nanoparticles on screen printed electrodes. *Electrochem. Commun.* **2013**, 33, 127–130.
- (53) Bharti, A.; Rana, S.; Dahiya, D.; Agnihotri, N.; Prabhakar, N. An electrochemical aptasensor for analysis of MUC1 using gold platinum bimetallic nanoparticles deposited carboxylated graphene oxide. *Anal. Chim. Acta* **2020**, *1097*, 186–195.
- (54) Zhang, J.; Ran, F.; Zhou, W.; Shang, B.; Yu, F.; Wu, L.; Hu, W.; He, X.; Chen, Q. Ultrasensitive fluorescent aptasensor for MUC1 detection based on deoxyribonuclease I-aided target recycling signal amplification. *RSC Adv.* **2018**, *8*, 32009–32015.